Available on the CERN CDS information server **CMS PAS SUS-13-003**

CMS Physics Analysis Summary

Contact: cms-pag-conveners-susy@cern.ch 2013/03/08

Search for stop in *R*-parity-violating supersymmetry with three or more leptons and b-tags

The CMS Collaboration

Abstract

We present a search for anomalous production of events with three or more isolated leptons and at least one bottom-quark jet produced in pp collisions at $\sqrt{s} = 8$ TeV. We analyze 19.5 fb^{-1} of data collected by the CMS experiment during the 2012 LHC run. No excesses above the standard model expectations are observed. We interpret the search results in the context of supersymmetric models with diminished missing transverse energy signatures arising from light stop pair production with *R*-parity-violating decays of the lightest supersymmetric particle.

1 Introduction

Supersymmetric (SUSY) extensions of the standard model (SM) offer a solution to the hierarchy problem and provide a mechanism for unifying particle interactions [1, 2]. Assigning R-parity fields as $R_{\mathrm{p}} = (-1)^{3B+L+2s}$, where B and L are baryon and lepton numbers, and s is the particle spin, all SM particle fields have $R_{\mathrm{p}} = +1$ while all superpartner fields have $R_{\mathrm{p}} = -1$. In models where R_{p} is conserved, superpartners can only be produced in pairs, and the lightest superpartner (LSP) is stable and a candidate for a dark matter particle. In addition, R_{p} conservation ensures proton stability. The role of R-parity in protecting the proton lifetime is an example of a more generalized matter symmetry, which applies also to theories besides SUSY wherein partner particles are posited.

Supersymmetric models with R-parity-violating (RPV) interactions conserving either B or L in addition to s can avoid direct contradiction with the proton-lifetime lower limits [3, 4]. The most general RPV renormalizable superpotential includes three trilinear R_{p} violating terms parametrized by the Yukawa couplings λ_{ijk}, λ'_{ijk}, and λ''_{ijk}.

$$W_{\not R_{\mathrm{p}}} = \frac{1}{2}\lambda_{ijk}L_iL_j\bar{E}_k + \lambda'_{ijk}L_iQ_j\bar{D}_k + \frac{1}{2}\lambda''_{ijk}\bar{U}_i\bar{D}_j\bar{D}_k,$$

where i, j, and k are generation indices, L and Q are the lepton and quark $SU(2)_L$ doublet superfields and $\bar{E}$, $\bar{D}$, and $\bar{U}$ are the charged lepton, down-like quark, and up-like quark $SU(2)_L$ singlet superfields. The third term violates baryon-number, while the first and second terms are lepton-number violating. In this analysis, we consider R-parity-violating interactions where one of the leptonic (λ_{ijk}) or semileptonic (λ'_{ijk}) couplings is non-zero and the rest are zero.

RPV interactions allow for single production of SUSY particles (sparticles) and for sparticle decay into SM particles only. Prior searches for RPV interactions in multilepton final states include those by the CDF and the D0 experiments at the Tevatron [5, 6] and those by H1 [7] and ZEUS [8], which have been superseded by the Compact Muon Solenoid (CMS) experiment [9, 10] and the ATLAS experiment at the Large Hadron Collider (LHC) [11].

SUSY models that focus on providing solutions to why the Higgs boson mass can be above the LEP-2 limit of $m_h > 114.4$ GeV [12] are referred to as natural SUSY models. These models are receiving renewed interest because of an apparent boson with mass near 125 GeV [13, 14]. Natural supersymmetry requires stop squarks, the top quark superpartners, be lighter than around a TeV. It is therefore worthwhile investigating signatures that arise from stop squark pair production over the full set of possibilities for stop decay modes, including through leptonic R-parity violating couplings. The introduction of RPV couplings does not preclude a natural hierarchy and can allow the constraints on the stop mass to be relaxed [15].

In RPV models, the LSP is unstable and a common experimental strategy of SUSY searches—selecting events with large missing transverse energy ($E_{\mathrm{T}}^{\mathrm{miss}}$) —is not optimal [3]. Instead, collecting all of the energy in the event provides better sensitivity to the mass scale of new particles. We use S_{T}, which is the scalar sum of $E_{\mathrm{T}}^{\mathrm{miss}}$, H_{T} and L_{T}, where H_{T} and L_{T} are the scalar sums of jet and charged lepton p_{T}, respectively. Besides being able to distinguish between different stop masses in our models, this variable also provides separation between signal and standard model backgrounds.

We present the result of a search for pair production of stop squarks with RPV decays of the lightest sparticle in multilepton events with one or more bottom-tagged jets. The data used in this analysis correspond to 19.5 fb^{-1} recorded in 2012 with the CMS detector at the LHC

producing proton-proton collisions at 8 TeV center-of-mass energy.

2 The CMS Detector

The CMS detector [16] has cylindrical symmetry around the pp beam axis with tracking and muon detectors within pseudorapidity $|\eta| < 2.4$. The tracking system, used to measure the trajectory and momentum of charged particles, consists of multilayered silicon pixel and strip detectors in a 3.8 Tesla solenoidal magnetic field. Particle energies are measured with concentric electromagnetic and hadronic calorimeters. Muon detectors consisting of wire chambers are at the outer radial edge of the detector. Data from pp interactions must satisfy the requirements of a two-level trigger system. The first level performs a fast selection for physics entities above a certain threshold. The second level performs a full event reconstruction.

3 Event Selection and Monte Carlo Simulation

We select events with three or more leptons and at least one bottom-tagged jet that are accepted by a trigger that requires at least two electrons and/or muons. We require that any opposite-sign, same-flavor (OSSF) pair of electrons or muons have an invariant mass $m_{\ell\ell} > 12$ GeV and that it is not in the range $75 < m_{\ell\ell} < 105$ GeV. These requirements remove low-mass bound states or $\gamma^* \to \ell^+\ell^-$ production and processes that produce signatures with Z bosons, respectively. We separate events using the number of reconstructed hadronically decaying taus. In each of our signal regions, we bin events based on their S_{T}.

Electrons and muons are reconstructed using quantities from the tracker, calorimeter, and muon systems. Details of reconstruction and identification can be found in Ref. [17] for electrons and in Ref. [18] for muons. We require that the leading electron or muon in each event have $p_T > 20$ GeV. Subsequent electrons and muons must have $p_T > 10$ GeV and all of them must have $|\eta| < 2.4$.

The hadronic decays of taus (τ_{h}) yield either a single charged track (one-prong) or three charged tracks (three-prong) occasionally with additional electromagnetic energy from neutral pion decays. Both one- and three-prong τ_{h} decays are used in this analysis if they have $p_{\mathrm{T}} > 20$ GeV, reconstructed using the hadron plus strips method [19].

To ensure that electrons, muons, and taus are isolated, we use the CMS particle-flow algorithm (PF) [20, 21] to identify the source of energy deposits in the trackers and calorimeters. We then sum the contribution in a cone of radius 0.3 in $\Delta R = \sqrt{\Delta\eta^2 + \Delta\phi^2}$ and subtract the lepton p_{T} to calculate E_{cone}. For electrons and muons, we correct for pileup contributions and divide the summed energy by the lepton p_{T} to find the relative isolation $I_{\mathrm{rel}} = E_{\mathrm{cone}}/p_{\mathrm{T}}$, which is required to be less than 0.15. For hadronic taus, we require that E_{cone} is less than 2 GeV after excluding contributions originating from the pileup vertices.

We use PF-reconstructed jets [22], using the anti-k_{T} algorithm [23] with a distance parameter of 0.5, that have $|\eta| < 2.5$ and $p_{\mathrm{T}} > 30$ GeV. Jets are required to be a distance $\Delta R > 0.3$ from any isolated electron, muon, or tau. To determine whether the jet originated from a bottom-quark we use the combined secondary vertex algorithm, which calculates a likelihood discriminant using track impact parameter and secondary vertex information. This discrimination selects heavy flavor jets with a high probability and suppresses light flavor jets [24].

Monte Carlo simulations are used to estimate the backgrounds of some SM processes and to understand the efficiency and acceptance of the new physics models we are investigat-

ing. The SM background samples are generated using the MADGRAPH event generator [25] with parton showering and fragmentation modeled using PYTHIA [26] and passed through a GEANT4-based [27] representation of the CMS detector. Signal samples are generated with MADGRAPH [15] and PYTHIA and passed through the CMS fast-simulation package [28]. Next-to-leading order, next-to-leading log cross sections and their uncertainties for the SUSY signal processes are calculated by the LHC SUSY cross sections working group [29–33].

4 Backgrounds

Multilepton signals have two main sources of backgrounds. The first source is processes that produce real multilepton events. The most significant examples are WZ and ZZ production, but rare processes such as $t\bar{t}W$ and $t\bar{t}Z$ can also contribute. The second is when an object is misidentified as a prompt isolated lepton when it is actually a misidentified hadron, lepton from a hadron decay (heavy or light flavored), or another source of fake leptons. The background estimation techniques are discussed in substantially more detail in Ref. [10].

We assess the contribution from standard model processes using simulated samples. For WZ and ZZ, which have substantial cross sections, these simulation samples have been validated in control regions. Our requirements of a bottom-quark jet and a Z-veto strongly reject both of these backgrounds. For rare processes, we rely solely on simulation.

Misidentified leptons are classified in three categories in our analysis: misidentified light leptons, misidentified hadronic taus, and light leptons originating from asymmetric internal conversions.

We estimate the contribution of misidentified light leptons by measuring the number of isolated tracks and applying a conversion factor between isolated leptons and isolated tracks. We measure this conversion factor in an on-Z control region, which we find to be $(0.9 \pm 0.2)\%$ for electrons and $(0.7 \pm 0.2)\%$ for muons. We apply the conversion factor to the sideband region with two light leptons and one isolated track. We adjust for the change in heavy-flavor content by determining the conversion factor as a function of the impact parameter distribution of non-isolated tracks. The contribution to this background from $t\bar{t}$ is taken directly from simulation. We assign an uncertainty of 50% to the $t\bar{t}$ contribution to our background estimates, which is driven by the low number of events in high-S_T control regions.

Similarly, the hadronic tau misidentification rate is measured in jet-dominated data by comparing the number of taus in the signal region with isolation $E_{\text{cone}} < 2$ GeV to the number in the sideband region $6 < E_{\text{cone}} < 30$ GeV. We measure this fake rate to have an average value of 15% and assign a systematic uncertainty of 30% based on variation in different control samples. We apply this fake rate to the sideband region with two light leptons and one sideband tau.

An internal conversion results from emission of a virtual photon that decays promptly in vacuum to a di-lepton pair. These conversions produce muons almost as often as electrons. In the case of asymmetric conversions, where one lepton has very low p_T and/or does not pass the selection criteria, Drell-Yan type processes with such conversions can lead to a significant background for three lepton signatures. This type of conversion is fundamentally different from external conversions resulting from interactions with detector material, which are not prompt and yield electrons rather than muons. External conversions are strongly suppressed by our electron identification requirements.

We measure the conversion factors in a control region devoid of new physics (low $E_{\text{T}}^{\text{miss}}$ and low H_{T}). The ratio of the number of $\ell^+\ell^-\ell^\pm$ on the Z peak to the number of $\ell^+\ell^-\gamma$ on the

Table 1: Observed yields for three and four lepton events from 19.5 fb^{-1} recorded in 2012. The channels are broken down by the total number of leptons (N_ℓ), the number of taus (N_τ), and the S_T. Expected yields are the sum of simulation and data-driven estimates of backgrounds in each channel. The channels are exclusive.

N_ℓ	N_τ	$0 < S_T < 300$		$300 < S_T < 600$		$600 < S_T < 1000$		$1000 < S_T < 1500$		$S_T > 1500$	
		obs	exp	obs	exp	obs	exp	obs	exp	obs	exp
4	0	0	0.186 ± 0.074	1	0.43 ± 0.22	0	0.19 ± 0.12	0	0.037 ± 0.039	0	0.000 ± 0.021
4	1	1	0.89 ± 0.42	0	1.31 ± 0.48	0	0.39 ± 0.19	0	0.019 ± 0.026	0	0.000 ± 0.021
3	0	116	123 ± 50	130	127 ± 54	13	18.9 ± 6.7	1	1.43 ± 0.51	0	0.208 ± 0.096
3	1	710	698 ± 287	746	837 ± 423	83	97 ± 48	3	6.9 ± 3.9	0	0.73 ± 0.49

Z peak defines the conversion factor, which is $0.5\% \pm 0.1\%$ ($2.1\% \pm 0.3\%$) for muons (electrons) [10]. The uncertainties are statistical only. We assign systematic uncertainties of 100% to these conversion factors from our underlying assumption of proportionality between virtual and on-shell photons as well as our inability to remove fake photons from sideband regions.

5 Systematic Uncertainties

On our simulation samples, signal and background, we apply a systematic of 4.4% to account for how well the luminosity of the data is known [34]. Our signal cross sections have varying uncertainty from 15% at 250 GeV stop mass to 51% at 1.5 TeV, which come from the parton distribution function uncertainties and the renormalization and factorization scale uncertainties [35]. We scale the WZ and ZZ simulation samples to match data in control regions. The overall systematic uncertainty on WZ and ZZ contributions to our signal regions varies between 15% and 30% depending on the kinematics, and is the combination of the normalization uncertainties with efficiency and resolution uncertainties. Our muon identification efficiency uncertainty is 11% at muon p_T of 10 GeV and 0.2% at 100 GeV. For electrons the uncertainties are 14% at 10 GeV and 0.6% at 100 GeV. The uncertainty on the efficiency of the bottom-quark tagger is 6%. The uncertainty on the E_T^{miss} resolution contributes a 4% uncertainty and the jet energy scale uncertainty contributes 0.5% in our background estimates [36]. We assign an uncertainty of 50% for the $t\bar{t}$ contribution to backgrounds. This estimate is driven by the low event counts in the isolation distributions in high S_T bins, which are used to validate the fake rate in the $t\bar{t}$ simulation sample. We apply a 50% uncertainty to the normalization of all rare processes that have not been measured.

6 Event Yields

We divide our events into four signal regions (SRs) with depending on whether there are three or four total leptons that include zero or one hadronic tau. We veto events in which any OSSF dilepton pair has an invariant mass in the Z window. Each SR is subsequently divided into 5 bin in S_T: [0-300], [300-600], [600-1000], [1000-1500] and [>1500] GeV. The different S_T bins are sensitive to the stop mass and the lepton flavors are sensitive to different RPV couplings. For example, the leptonic RPV λ_{122} yields final states with electrons and muons, while λ_{233} yields final states with taus. The definitions of the signal regions and the observed and expectations are shown in Table 1. We also show the S_T distributions for the four signal regions in Fig. 1 with the background expectations from different sources shown separately. Agreement with standard model predictions in our signal regions is very good.

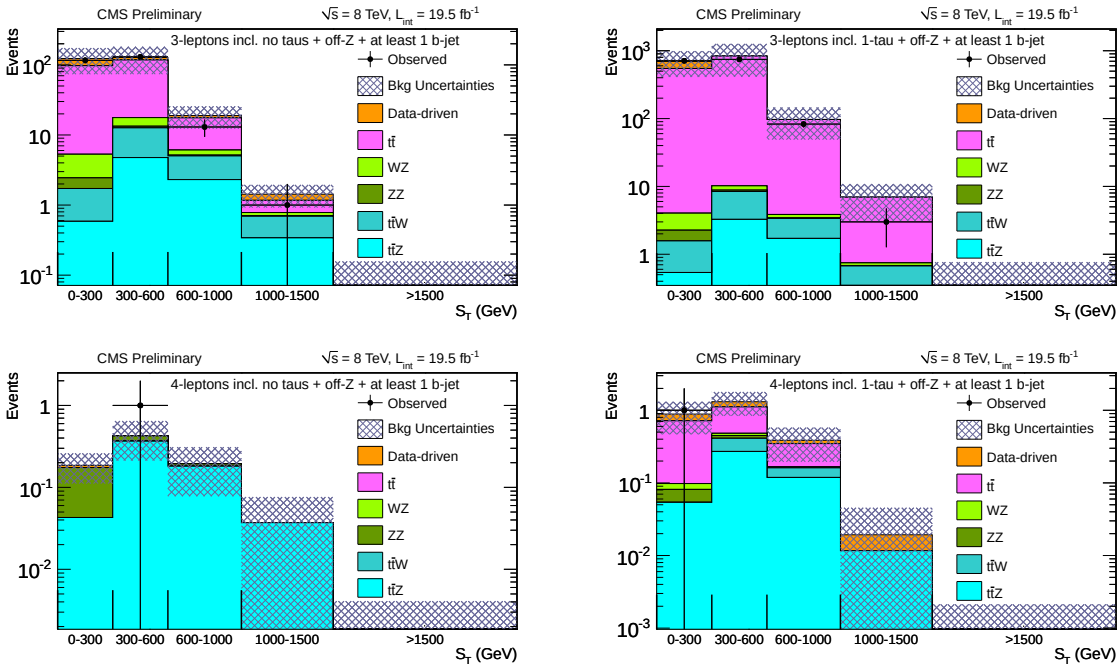

Figure 1: S_{T} distributions for each of the four categories of multilepton events including observed yields and background contributions. The top row contains the distributions for events with three leptons and the bottom row contains the distributions for events with four leptons. The left plots corresponds to events with no hadronically-decaying taus and the right plots contain events with taus. In these figures, the data-driven component of the background estimate refers to the result we get from applying our procedure to determine how many misidentified leptons enter our signal regions.

Table 2: Observed yields for three and four lepton events that contain either an on-Z OSSF dilepton pair or no b-tagged quarks or both. The channels are exclusive.

N_ℓ	N_τ	$600 < S_T < 1000$		$1000 < S_T < 1500$		$S_T > 1500$	
		obs	exp	obs	exp	obs	exp
4	0	5	8.2 ± 2.6	2	0.96 ± 0.37	0	0.113 ± 0.056
4	1	2	3.8 ± 1.3	0	0.34 ± 0.16	0	0.040 ± 0.033
3	0	165	174 ± 53	16	21.4 ± 8.4	5	2.18 ± 0.99
3	1	276	249 ± 80	17	19.9 ± 6.8	0	1.84 ± 0.83

We gain additional sensitivity in regions where the top quark is off-shell by relaxing the b-tag and on/off-Z requirements for events with $S_T > 600$ GeV. The results for these channels are shown in Table 2, which contain events that have either an OSSF dilepton pair with a mass in the Z window or no b-tagged quarks or both.

7 Limits on models of new physics

To demonstrate how natural SUSY might manifest itself with RPV couplings, we examine a stop RPV model. Fig. 2 shows the schematic of the production and decay mechanism for this simplified model.

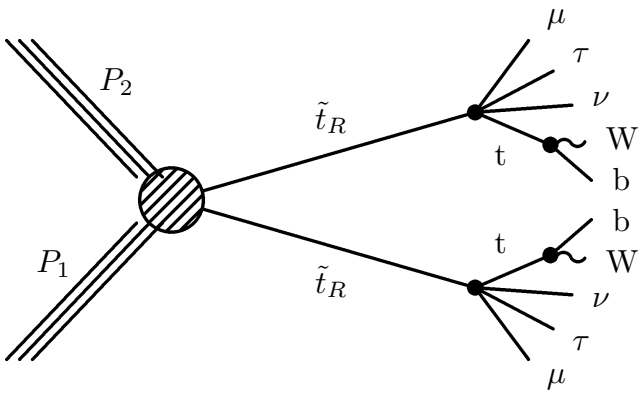

Figure 2: Right-handed stop pair production and decay topology in proton-proton collisions with a λ_{ijk} RPV coupling leading to a final state with at least four leptons, where $L_iL_j = \nu_i\ell_j - \ell_i\nu_j$. Left- and right-handed slepton masses are 200 GeV heavier than the bino mass, with all other super partners decoupled. Production and decay topology with a λ'_{ijk} RPV coupling is similar with L_j replaced by Q_j, and $L_iQ_j = \nu_i d_j - \ell_i u_j$.

In this model, the stop decays to a top quark and intermediate on or off shell bino, $\widetilde{t}_R \to \widetilde{\chi}_1^{0*} + t$. The intermediate bino then decays to two leptons and a neutrino through the leptonic R-parity violating interaction, $\widetilde{\chi}_1^{0*} \to \ell_i + \nu_j + \ell_k$ and $\nu_i + \ell_j + \ell_k$ or through the semi-leptonic R-parity violating interaction, $\widetilde{\chi}_1^{0*} \to \ell_i + q_j + q_k$ and $\nu_i + q_j + q_k$.

We generate mass spectra to benchmark models with the leptonic RPV couplings λ_{122} or λ_{233} non-zero with stop masses 900-1200 in 100 GeV steps and bino masses 100-1300 in 400 GeV steps. In a model with the semi-leptonic RPV coupling λ'_{233} non-zero, we use stop masses 300-1000 in 50 GeV steps and bino masses 200-850 in 50 GeV steps. In both cases, slepton and neutrino masses are 200 GeV above the bino mass. Other particles are decoupled.

The method used to calculate our limits is described in detail in Ref. [10]. The channels used to

Table 3: Kinematically allowed stop decay modes with RPV coupling λ'_{233}. The allowed neutralino decay modes for $m_t < m_{\widetilde{\chi}^0_1} < m_{\widetilde{t}}$ are $\widetilde{\chi}^0_1 \to \mu t\bar{b} + \nu b\bar{b}$.

region label	kinematic region	stop decay mode(s)
A	$m_t < m_{\widetilde{t}} < 2m_t, m_{\widetilde{\chi}^0_1}$	$\widetilde{t} \to t\nu b\bar{b}$
B	$2m_t < m_{\widetilde{t}} < m_{\widetilde{\chi}^0_1}$	$\widetilde{t} \to t\mu t\bar{b} + t\nu b\bar{b}$
C	$m_{\widetilde{\chi}^0_1} < m_{\widetilde{t}} < m_W + m_{\widetilde{\chi}^0_1}$	$\widetilde{t} \to \ell\nu b\widetilde{\chi}^0_1 + jjb\widetilde{\chi}^0_1$
D	$m_W + m_{\widetilde{\chi}^0_1} < m_{\widetilde{t}} < m_t + m_{\widetilde{\chi}^0_1}$	$\widetilde{t} \to Wb\widetilde{\chi}^0_1$
E	$m_t + m_{\widetilde{\chi}^0_1} < m_{\widetilde{t}}$	$\widetilde{t} \to t\widetilde{\chi}^0_1$

find the limits are more fine-grained than those shown in Tables 1 and 2.

For all of the couplings, we expect two bottom-quark jets and up to two leptons from the two top quarks. For the leptonic RPV coupling λ_{122}, we also expect four electrons or muons. For leptonic coupling λ_{233}, we expect four leptons with up to two muons and the rest taus. The taus can decay leptonically or hadronically. For the semi-leptonic coupling λ'_{233}, we expect up to two muons, as well as two top quarks and two bottom quarks.

In the LLE models, we find that the limits are approximately independent of the bino mass, and we are able to exclude models with stop mass below approximately 1100 GeV when λ_{122} is non-zero and below 900 GeV when λ_{233} is non-zero. These limits are shown in the first two rows of Fig. 3, respectively. There is a change in kinematics at the line $m_{\widetilde{t}} = m_{\widetilde{\chi}^0_1} + m_t$, below which the stop decay is two-body and above which the stop decay is four-body. Near this line, the $\widetilde{\chi}^0_1$ and top are produced almost at rest, which results in soft leptons, reducing our acceptance. This loss of acceptance is more pronounced in λ_{233} and causes the loss of observed sensitivity in that model near that line.

In the LQD model, which has non-zero λ'_{233}, the kinematics of the decay are more complicated. These different kinematic regions are described in Table 3. The most significant effect is when the decay $\chi^0_1 \to \mu + t + b$ is kinematically disfavored, which reduces the number of available leptons. The different regions where this effect is pronounced drive the shape of the exclusion for λ'_{233}. The region inside the curve is excluded.

8 Conclusions

We have performed a search for RPV supersymmetry using a variety of multilepton final states using data corresponding to 19.5 fb^{-1} recorded in 2012 with the CMS detector at the LHC producing proton-proton collisions at 8 TeV center-of-mass energy. We see good agreement between observations and SM expectations. We show limits on the stop mass for models with LLE RPV couplings λ_{122} and λ_{233} and for LQD RPV coupling λ'_{233}.

References

[1] H. P. Nilles, "Supersymmetry, Supergravity and Particle Physics", *Phys. Rept.* **110** (1984) 1, doi:10.1016/0370-1573(84)90008-5.

[2] H. E. Haber and G. L. Kane, "The Search for Supersymmetry: Probing Physics Beyond the Standard Model", *Phys. Rept.* **117** (1985) 75, doi:10.1016/0370-1573(85)90051-1.

[3] R. Barbier et al., "R-parity violating supersymmetry", *Phys. Rept.* **420** (2005) 1–202, doi:10.1016/j.physrep.2005.08.006, arXiv:hep-ph/0406039.

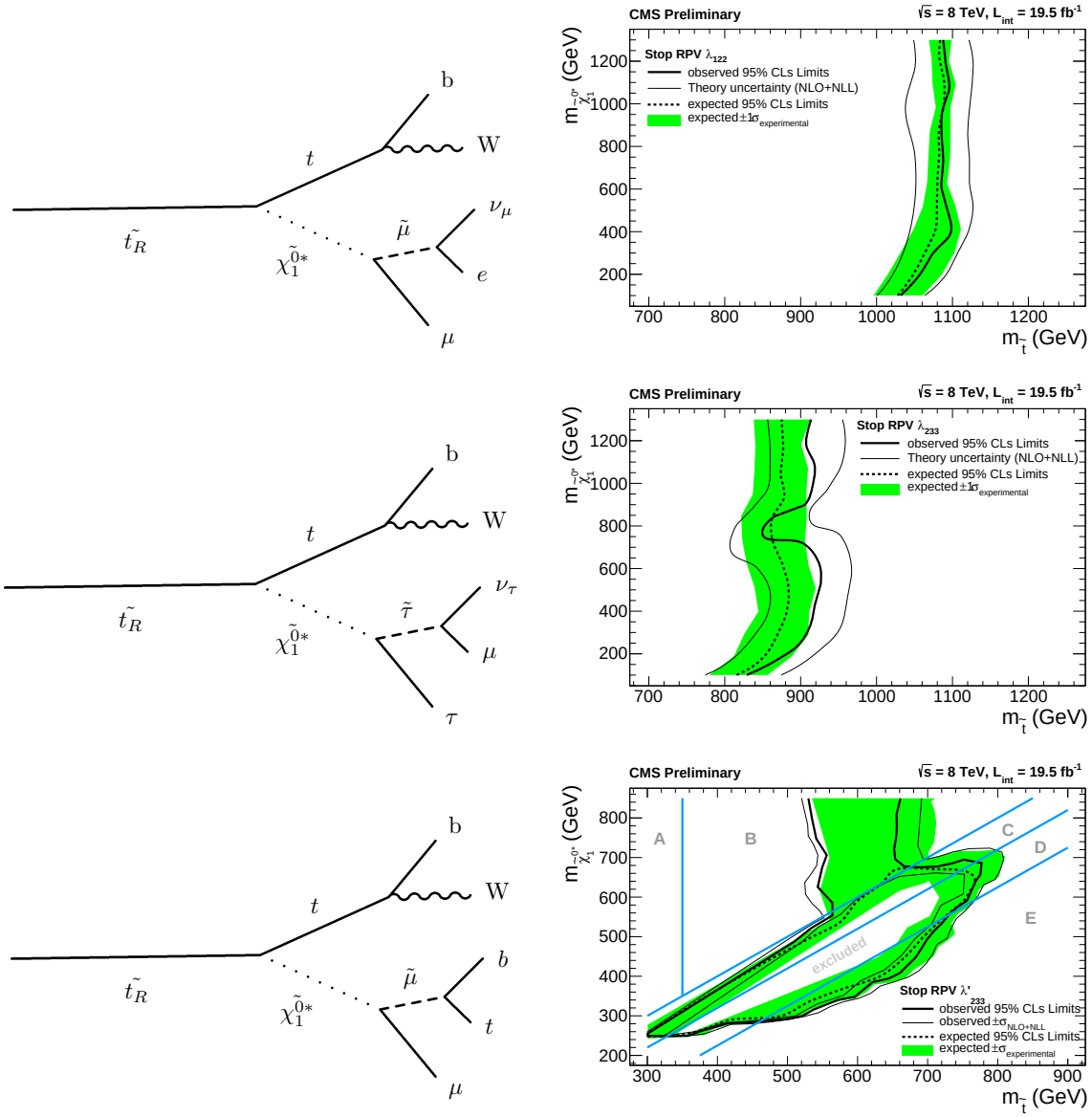

Figure 3: 95% CL limits for stop mass in models with RPV couplings λ_{122}, λ_{233}, and λ'_{233} with diagrams of the relevant RPV decays. For the couplings λ_{122} and λ_{233}, the region to the left of the curve is excluded. For λ'_{233}, the region inside the curve is excluded. The different regions on the λ'_{233} exclusion correspond to regions where the stop decays to different products and are explained in Table 3.

[4] Particle Data Group Collaboration, "Review of particle physics", *J. Phys.* **G37** (2010) 075021, doi:10.1088/0954-3899/37/7A/075021.

[5] D0 Collaboration, "Search for R-parity violating supersymmetry via the $LL\overline{E}$ couplings λ_{121}, λ_{122} or λ_{133} in $p\bar{p}$ collisions at $\sqrt{s}$ = 1.96-TeV", *Phys. Lett.* **B638** (2006) 441, doi:10.1016/j.physletb.2006.05.077.

[6] CDF Collaboration, "Search for anomalous production of multilepton events in $p\bar{p}$ collisions at $\sqrt{s}$ = 1.96-TeV", *Phys. Rev. Lett.* **98** (2007) 131804, doi:10.1103/PhysRevLett.98.131804.

[7] H1 Collaboration, "A search for squarks of Rp-violating SUSY at HERA", *Zeitschrift für Physik C Particles and Fields* **71** (1996) doi:10.1007/BF02906978.

[8] ZEUS Collaboration, "Search for stop production in R-parity-violating supersymmetry at HERA", *The European Physical Journal C* **50** (2007) 269–281, doi:10.1140/epjc/s10052-007-0240-8.

[9] CMS Collaboration, "Search for Physics Beyond the Standard Model Using Multilepton Signatures in pp Collisions at sqrt(s)=7 TeV", arXiv:1106.0933.

[10] CMS Collaboration, "Search for anomalous production of multilepton events in pp collisions at sqrt(s)=7 TeV", *JHEP* **1206** (2012) 169, doi:10.1007/JHEP06(2012)169, arXiv:1204.5341.

[11] ATLAS Collaboration, "Search for R-parity-violating supersymmetry in events with four or more leptons in $\sqrt{s} = 7$ TeV pp collisions with the ATLAS detector", *JHEP* **1212** (2012) 124, doi:10.1007/JHEP12(2012)124, arXiv:1210.4457.

[12] LEP Working Group for Higgs boson searches, ALEPH Collaboration, DELPHI Collaboration, L3 Collaboration, OPAL Collaboration Collaboration, "Search for the standard model Higgs boson at LEP", *Phys.Lett.* **B565** (2003) 61–75, doi:10.1016/S0370-2693(03)00614-2, arXiv:hep-ex/0306033.

[13] CMS Collaboration, "Observation of a new boson at a mass of 125 GeV with the CMS experiment at the LHC", *Phys.Lett.* **B716** (2012) 30–61, doi:10.1016/j.physletb.2012.08.021, arXiv:1207.7235.

[14] ATLAS Collaboration Collaboration, "Observation of a new particle in the search for the Standard Model Higgs boson with the ATLAS detector at the LHC", *Phys.Lett.* **B716** (2012) 1–29, doi:10.1016/j.physletb.2012.08.020, arXiv:1207.7214.

[15] J. A. Evans and Y. Kats, "LHC Coverage of RPV MSSM with Light Stops", arXiv:1209.0764.

[16] CMS Collaboration, "The CMS experiment at the CERN LHC", *JINST* **0803** (2008) S08004, doi:10.1088/1748-0221/3/08/S08004.

[17] CMS Collaboration, "Electron reconstruction and identification at $\sqrt{s}$ = 7 TeV", *CMS Physics Analysis Summary* **CMS-PAS-EGM-10-004** (2010).

[18] CMS Collaboration, "Performance of muon identification in pp collisions at $\sqrt{s}$ = 7 TeV", *CMS Physics Analysis Summary* **CMS-PAS-MUO-10-002** (2010).

[19] CMS Collaboration, "Performance of τ-lepton reconstruction and identification in CMS", *Journal of Instrumentation* **7** (2012), no. 1, P01001.

[20] CMS Collaboration, "Study of tau reconstruction algorithms using pp collisions data collected at $\sqrt{s}$ = 7 TeV", *CMS Physics Analysis Summary* **CMS-PAS-PFT-10-004** (2010).

[21] CMS Collaboration, "CMS Strategies for tau reconstruction and identification using particle-flow techniques", *CMS Physics Analysis Summary* **CMS-PAS-PFT-08-001** (2010).

[22] CMS Collaboration, "Commissioning of the Particle-Flow Reconstruction in Minimum-Bias and Jet Events from pp Collisions at 7 TeV", *CMS Physics Analysis Summary* **CMS-PAS-PFT-10-002** (2010).

[23] M. Cacciari, G. P. Salam, and G. Soyez, "The anti-k_t jet clustering algorithm", *JHEP* **04** (2008) 063, doi:10.1088/1126-6708/2008/04/063, arXiv:0802.1189.

[24] CMS Collaboration, "b-Jet Identification in the CMS Experiment",.

[25] F. Maltoni and T. Stelzer, "MadEvent: Automatic event generation with MadGraph", *JHEP* **02** (2003) 027, doi:10.1088/1126-6708/2003/02/027.

[26] T. Sjöstrand, S. Mrenna, and P. Skands, "A Brief Introduction to PYTHIA 8.1", *Comput. Phys. Commun.* **178** (2008) 852, doi:10.1016/j.cpc.2008.01.036.

[27] GEANT4 Collaboration, "GEANT4: A simulation toolkit", *Nucl. Instrum. Meth.* **A506** (2003) 250, doi:10.1016/S0168-9002(03)01368-8.

[28] CMS Collaboration, "Fast Simulation of the CMS Detector", *CMS Conference Report* (2009).

[29] W. Beenakker et al., "Production of charginos, neutralinos, and sleptons at hadron colliders", *Phys. Rev. Lett.* **83** (1999) 3780, doi:10.1103/PhysRevLett.83.3780.

[30] A. Kulesza and L. Motyka, "Threshold resummation for squark-antisquark and gluino-pair production at the LHC", *Phys.Rev.Lett.* **102** (2009) 111802, doi:10.1103/PhysRevLett.102.111802, arXiv:0807.2405.

[31] A. Kulesza and L. Motyka, "Soft gluon resummation for the production of gluino-gluino and squark-antisquark pairs at the LHC", *Phys.Rev.* **D80** (2009) 095004, doi:10.1103/PhysRevD.80.095004, arXiv:0905.4749.

[32] W. Beenakker et al., "Soft-gluon resummation for squark and gluino hadroproduction", *JHEP* **0912** (2009) 041, doi:10.1088/1126-6708/2009/12/041, arXiv:0909.4418.

[33] W. Beenakker et al., "Squark and Gluino Hadroproduction", *Int.J.Mod.Phys.* **A26** (2011) 2637–2664, doi:10.1142/S0217751X11053560, arXiv:1105.1110.

[34] CMS Collaboration, "Absolute Calibration of the Luminosity Measurement at CMS: Winter 2012 Update", *CMS Physics Analysis Summary* (2012).

[35] M. Kramer et al., "Supersymmetry production cross sections in pp collisions at $\sqrt{s}$ = 7 TeV", arXiv:1206.2892.

[36] CMS Collaboration, "Determination of jet energy calibration and transverse momentum resolution in CMS", *Journal of Instrumentation* **6** (2011), no. 11, P11002.